Influence of Rotor Design on Variable Reluctance Machine Torque

KARIMA CHALLAL*, MEHDI ABDELLAH*, HASSANE MOHELLEBI**
*Laboratory of Electromagnetic systems, **Electrotechnics Department
*Polytechnics school Algiers, **Tizi-Ouzou University
*BP 17, Bordj-El-Bahri, Algiers; **BP 17 RP Tizi-Ouzou University, 15000
ALGERIA

Abstract:- This paper describes the design of a variable reluctance machine with salient poles on both the rotor and stator. The latter comprises four poles. The work presented thereafter was undertaken with the aim of optimizing the machine torque. As a matter of fact, the study is based on the search of the architecture and the shape of the rotor leading to an optimum torque. The magnetic characteristics of material constituting the rotor were taken into account. The study was focused on the optimization of the difference between inductances, in conjunction and in opposition, which is finally, the image of the torque. Two kinds of rotors are considered: the first is massive and the second is laminated and made of alternate ferromagnetic and non-magnetic layers.

Key-Words: Reluctance networks, Variable reluctance machine, Doubly salient, Massive and laminated rotor, Optimal inductance, Machine torque, Flux2D software.

1 Introduction

A switched variable reluctance machine (VRM) has salient poles on both the rotor and stator, but only the latter has windings.

Torque is produced by the rotor tendency to turn to a position that minimizes the reluctance of the magnetic circuit energized by the stator windings [1]. So the torque production is due to the fact that inductances of stator coils are function of the rotor angular position [2].

The objective of this study is to search an optimal configuration of a doubly salient 4/2 VRM rotor (figure 1). To realize this machine we have used a continuous current machine stator as an inductor of variable reluctance machine. A progressive approach is adopted in the design and the rotor dimensioning. This results in the study of two rotor prototypes (the massive rotor and the laminated rotor with five layers) with the aim of improving the torque of the machine.

The appreciation parameter of the VRM torque is the ratio of inductances, direct and in quadrate. The latter are function of the form, dimensions and the material nature of the rotor.

For the search of an optimal rotor shape, we carried out an analytical calculation based on the magnetic circuit model representation of the machine. This calculation is supported by the analysis of the magnetic behavior of the machine using 'FLUX2D' software.

2 Description of the rotors

The massive rotor is made of XC38 steel with permeability less than those of the other ferromagnetic materials (μr=400) [3].

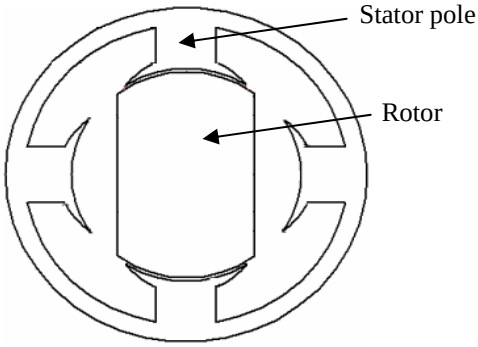

Fig. 1: 4/2 VRM with massive rotor

The laminated multi-layer rotor is made of alternate packets of ferromagnetic and non-magnetic sheets [4]. The ferromagnetic layers are composed of low thickness (0,35mm), iron-silicon, anisotropy sheets with a relatively significant permeability (μr=10000) [5] this will allow us to increase the inductance in conjunction position (L_c). So, the latter must correspond to the transversal axis of the rotor and should have a relatively significant permeability (μr=10000). For the layers of non-magnetic material, we used Teflon. The latter has the magnetic properties of the air which will contribute to the reduction of the inductance phase (L_o) for opposition state of the rotor.

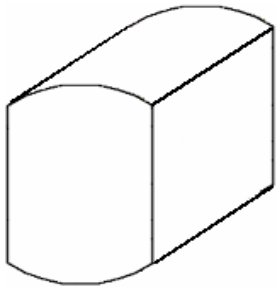

Fig. 2: Massive rotor representation of a VRM**.**

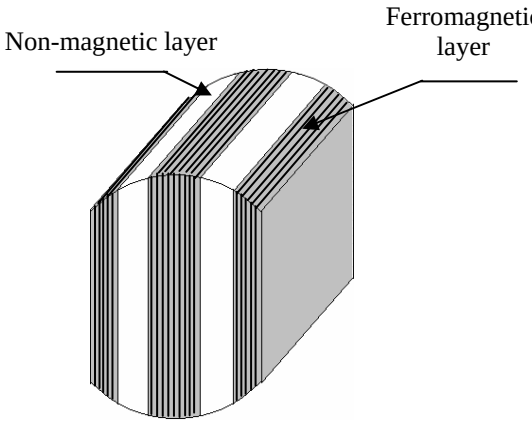

Fig. 3: Representation of the VRM alternate rotor with five layers

The two rotor prototypes, the massive and the alternate layers ferromagnetic (five layers), proposed in this study are represented on figures 2 and 3.

On Table 1 are presented the various parameters of the machine.

Table 1: Machine parameters

Parameters	**values**
External diameter of the machine (D_{ext})	149,7 mm.
Machine Length (L_N)	35,7 mm.
Rotor Diameter (D_{rot})	94 mm.
Air-gap (e)	0,5 mm.
Width of massive rotor (l_1)	56,56 mm.
Width of laminated rotor (l_2)	56,56 mm.
Rotor pole opening (β_r)	74°
Stator pole opening (β_s)	67°

3 Analytical method

We present here a design methodology that we developed for various electromagnetic structures. This methodology is based primarily on the use of a fast model of dimensioning which allows to a good calculation of performances. A present methodology is applied to an optimized design of a (4/2) variable reluctance machine.

To this end, a model of reluctance networks is developed for the preliminary dimensioning of this type of actuator.

The method of reluctance network is based on a geometrical simplification and a morphological decomposition of the magnetic circuit constituting the machine [6], [7].

However, when magnetic saturation is taken into account, and identification of the reluctances is well conducted, it provides very quickly good quality results [8]. Thus this method will be applied to the various proposed prototypes. Phase inductances for various rotor positions are given after having computed the reluctance's.

The representation of the machine by its reluctance network is illustrated by figure 4.

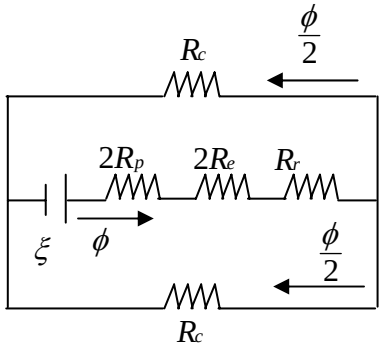

Fig. 4 : Magnetic circuit model of the machine

$$R_i = \frac{l_i}{\mu_i . s_i} \quad (1)$$

Where μ_i is the magnetic permeability, l_i is the length of the element crossed by flux, s_i is its average section and R_i are the different elements reluctance.

The determination of the reluctances will enable us to know the evolution of the phase inductance of the machine during the rotation of the mobile part. The phase inductance is calculated by the following formula:

$$L = \frac{N^2}{R} \quad (2)$$

where N is the inductor coils turns, L (H) is the phase inductance and R is the equivalent reluctance of the machine.

The curves of inductance variation according to the rotor position for the two rotors types are then analytically computed and presented on figures 5 and 6.

These curves show that the phase inductance grows, from its minimal value that corresponds to the no-aligned position of the rotor with the excited phase to its maximal value corresponding to the aligned position of the rotor with the axis of the excited phase, then it decrease from this maximum to the minimum.

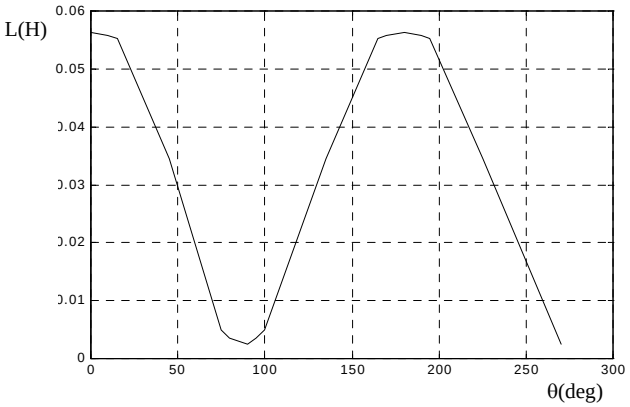

Fig. 5: Variation of the phase inductance according to the rotor position (VRM with massive rotor)

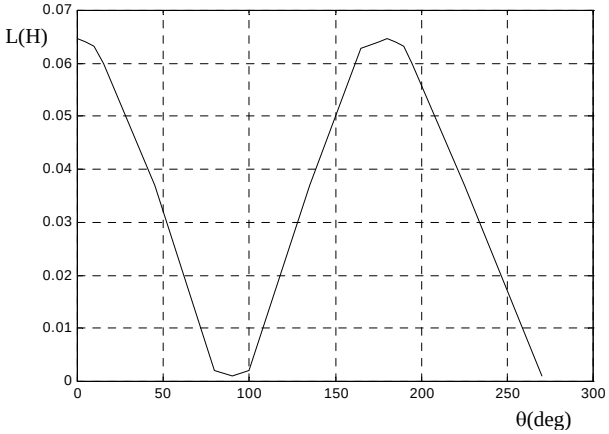

Fig. 6: Variation of the phase inductance according to rotor position (Alternated rotor of VRM with 5 layers)

These curves show that the phase inductance grows, from its minimal value that corresponds to the no-aligned position of the rotor with the excited phase to its maximal value corresponding to the aligned position of the rotor with the axis of the excited phase, then it decrease from this maximum to the minimum.

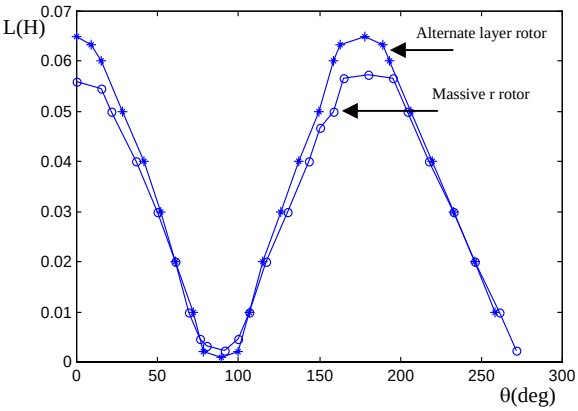

Fig.7: Inductance variation according to the rotor position

It should be noted that the variation of this inductance from one position to another is at the origin of the torque creation.

The confrontation in terms of inductance variation according to the rotor position the two rotor types are then presented on Fig.7.

We record a ratio of salient (L_c/L_o) of the order of:

- 22 for the massive rotor.
- 64 for the laminated rotor with five layers.

The torque can be formulated in the following expression:

$$C_e = \frac{k}{L_q}\left(\frac{L_d}{L_q} - 1\right) \qquad (3)$$

with k is a constant.

The improvement of the torque is shown below:

	L_d	L_q	L_d/L_q	C_e
Rotor with flat part	0.0564	0.0025	22	8400.k
Rotor with five layers	0.0646	0.001	64	63000.k

Table 2

4 Analysis of the VRM by Flux2D

The FLUX2D software was actually used as a design assistance tool to support analytical calculation. The software allowed us to establish the representation of the machine magnetic configuration and the evolution of magnetic flux density in the air-gap when the

rotor occupies particular positions, in conjunction and opposition, figures 8 and 9.

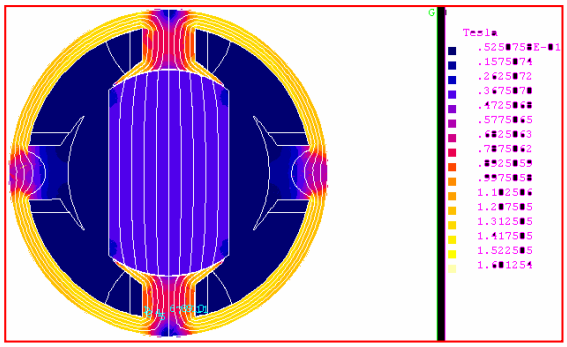

Fig. 8a: Flux density distribution of VRM with massive rotor (rotor in position of conjunction)

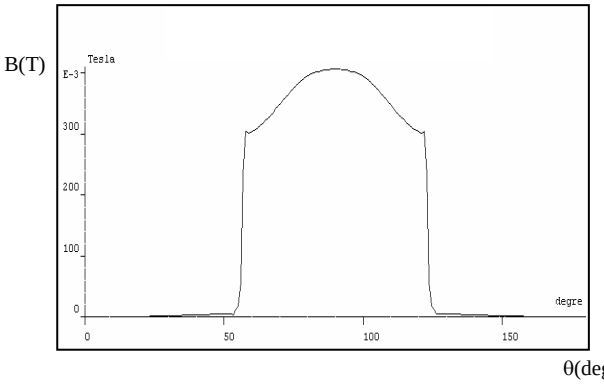

Fig. 8b: Flux density modulus in the air-gap of VRM with massive rotor (rotor in position of conjunction)

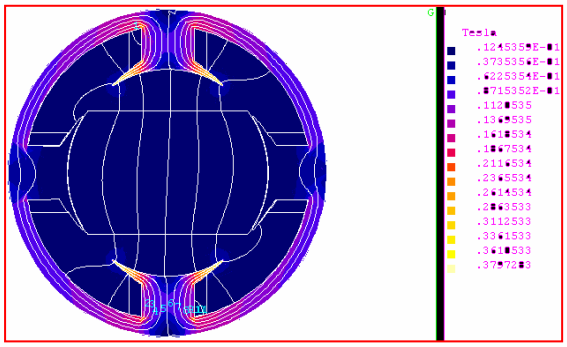

Fig. 8c: Flux density distribution of VRM with massive rotor (rotor in position of opposition)

We note for the position of conjunction shown on figures 8a, 9a a concentration of the field lines in the pole center.

This observation is illustrated on the curves of magnetic flux density distribution in the air-gap shown on the figure 8b, 9b by a high forehead in the medium of the curve. This high forehead corresponds to a value of flux density equal to 0,37 Tesla for the salient rotor poles and 0,78 Tesla for the rotor of five layers.

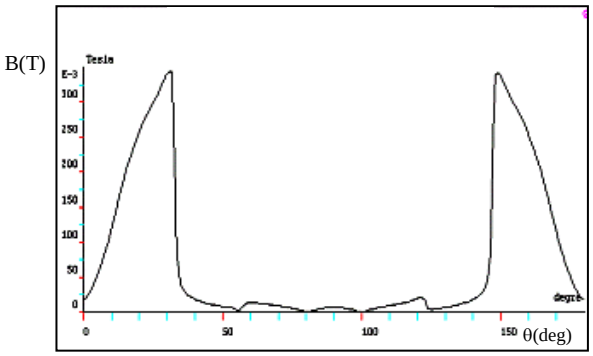

Fig. 8d: Flux density modulus in the air-gap of VRM with massive rotor (rotor in position of opposition)

The magnetic flux density distribution in the air-gap translates the geometrical shape of the poles in the case of the VRM with massive rotor figure 8b, and the structure of the rotor in the case of the VRM with laminated rotor figure 9b.

We note also a better distribution of flux density under the pole arc in the case of the massive rotor. The low values of flux density (figure 8d and 9d) in the air-gap relating to the position of opposition of the rotor reflect the low value of inductance L_o.

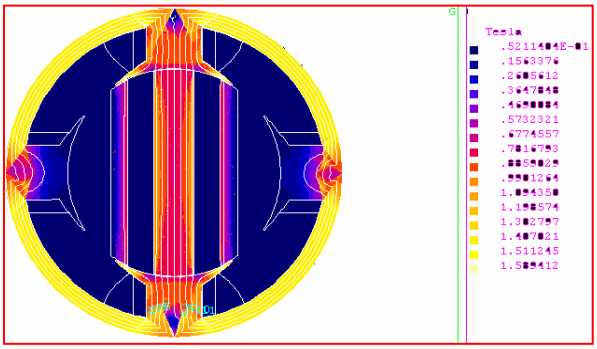

Fig. 9a: Flux density distribution of VRM with rotor of 5 layers (rotor in position of conjunction)

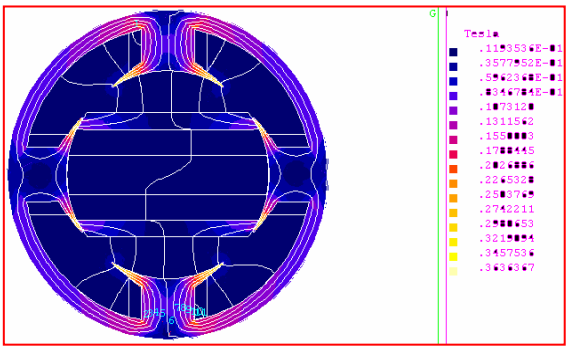

Fig. 9c: Flux density distribution of VRM rotor with 5 layers (rotor in position of opposition)

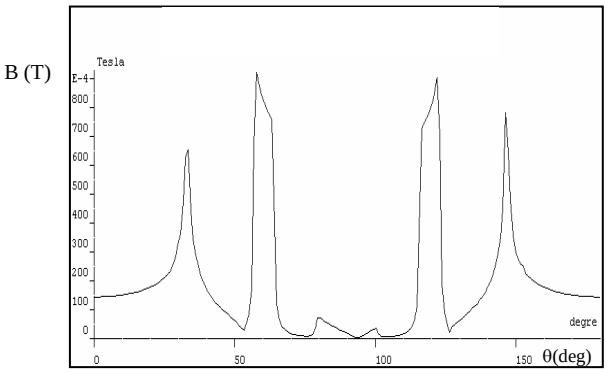

Fig. 9d : Flux density modulus in the air-gap of VRM rotor with 5 layers (rotor in position of opposition)

The magnetic flux density variation in the air-gap for different positions of the rotors corresponding to massive and laminated layers rotors is shown on Fig.10.

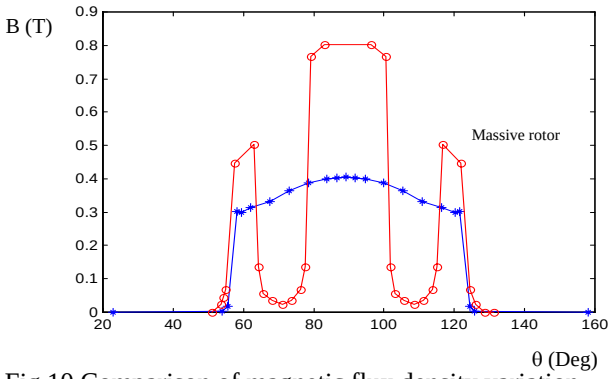

Fig.10.Comparison of magnetic flux density variation with rotor position (Massive and Laminated rotor)

Figure 10 shown that the higher value (B=0,78 T) of flux density corresponds to a rotor of five layers when the massive rotor induces only 0,37 T in air-gap. The curves of phase inductance variation according to the rotor position shown on figures 11, 12 enforce the validity of the results obtained analytically (Fig.5, Fig.6).

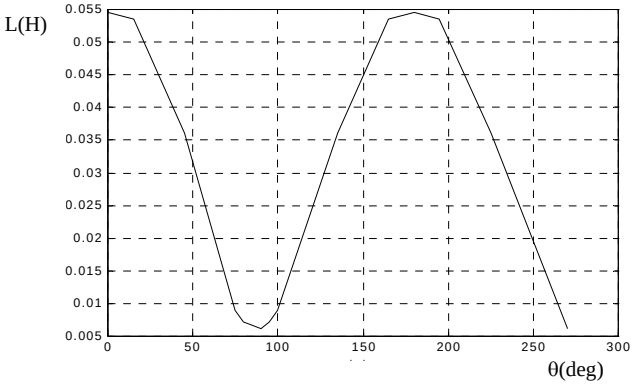

Fig. 11: Phase inductance variation according to the rotor position (VRM with massive rotor)

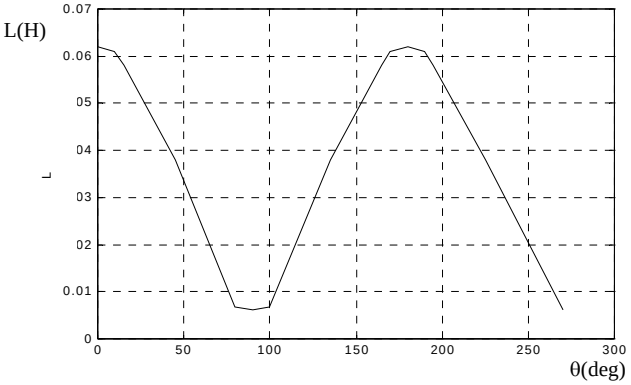

Fig. 12: Phase inductance variation according to the rotor position (VRM alternated rotor with 5 layers)

5 Conclusion

Lamination of the rotor of a variable reluctance machine contributes clearly to the improvement of the torque in comparison with that of the massive rotor.

The judicious choice of material constituting the rotor, the anisotropic Fe-silicon in our case, made it possible to increase the phase inductance when the rotor is in position of conjunction and to improve the level of induction in the air-gap.

The waveform of air-gap magnetic flux density for the case of the laminated rotor can be improved by an increase of the ferromagnetic layer number.

References:

[1] J D Wale and C Pollock, Novel converter topologies for a two-phase switched reluctance motor with fully pitched windings, *IEEE Transactions On Magnetics*, 1996, pp. 1798-1803.

[2] C. Kingsley, S. D. Umans**,** *Electric Machinery*, International Edition, 1991.

[3] M. Abdellah, Y. Matriche, K. Challal, H. Mohellebi, Computer's conception assisted of variable reluctance machine rotor with smooth stator, 2006 IEEE Mediterranean Electrotechnical conference, MELECON 2006, May 16-19, Benalmadena (Malaga), Spain, pp.1162-1165.

[4] H. Hofmann, S. R. Sanders, Synchronous Reluctance Motor/Alternator for Flywheel Energy Storage Systems, *Department of Electrical Engineering and Computer Science University of California, Berkeley*.

[5] P. Brissonneau**,** Magnétisme et Matériaux Magnétiques pour l'Electrotechnique, *Hermès Paris*, 1997.

[6] M. Geoffroy, B. Multon, E. Houang, R.Neji, Couplage de méthodes pour le calcul rapide des caractéristiques électromagnétiques des machines à réluctance variable à double saillance, *Colloque méthodes informatiques de la conception industrielle*, ESIM Marseille,18 juin 1993, pp.81-90.

[7] P. Vijayraghavan, Design of Switched Reluctance Motors and Development of a Universal Controller for Switched Reluctance and Permanent Magnet Brushless DC Motor Drives, *PhD in Electrical Engineering*, November 15, 2001.

[8] L. El Amraoui, Conception électromécanique d'une gamme d'actionneurs linéaire tubulaire à réluctance variable, *Thèse de doctorat*, 18-12-2002.